Multiscale Systems Biology and Physics of Thrombosis Under Flow

M. H. Flamm and S. L. Diamond

Department of Chemical and Biomolecular Engineering, Institute for Medicine and Engineering, 1024 Vagelos Research Laboratory, University of Pennsylvania, Philadelphia, PA 19104, USA

Associate Editor Michael R. King oversaw the review of this article.

Abstract—Blood clotting under hemodynamic conditions involves numerous multiscale interactions from the molecular scale to macroscopic vessel and systemic circulation scales. Transmission of shear forces to platelet receptors such as GPIbα, P-selectin, $\alpha_2\beta_1$, and $\alpha_{2b}\beta_3$ controls adhesion dynamics. These forces also drive membrane tether formation, cellular deformation, and mechanosignaling in blood cells. Blood flow results in red blood cell (RBC) drift towards the center of the vessel along with a near-wall plasma layer enriched with platelets. RBC motions also dramatically enhance platelet dispersion. Trajectories of individual platelets near a thrombotic deposit dictate capture–activation–arrest dynamics as these newly arriving platelets are exposed to chemical gradients of ADP, thromboxane, and thrombin within a micron-scale boundary layer formed around the deposit. If shear forces are sufficiently elevated (>50 dyne/cm^2), the largest polymers of von Willebrand Factor may elongate with concomitant shear-induced platelet activation. Finally, thrombin generation enhances platelet recruitment and clot strength *via* fibrin polymerization. By combination of coarse-graining, continuum, and stochastic algorithms, the numerical simulation of the growth rate, composition, and occlusive/embolic potential of a thrombus now spans multiscale phenomena. These simulations accommodate particular flow geometries, blood phenotype, pharmacological regimen, and reactive surfaces to help predict disease risk or response to therapy.

Keywords—Thrombosis, Platelet, Hemodynamic, Coagulation, Adhesion.

INTRODUCTION

Human blood is a multicellular "organ" whose function is influenced by prevailing hemodynamic forces. Blood is easily obtained for diagnostic uses and can be subjected to automated high throughput liquid handling and microfluidic experimentation. During a clotting event, platelets display combinatorial signaling through the GPVI receptor and multiple G-protein coupled receptors (GPCR) with outside–in/inside–out signaling pathways that trigger shape change, integrin activation, granule release, and phosphatidylserine exposure (see Li *et al.*[44] for review). Importantly, metabolic pathways in platelets are decoupled from changes in gene expression since platelets have no nucleus. Extracellular processes involving serine protease cascades and their associated reaction topology and kinetics are fairly well defined for coagulation, fibrinolysis, and complement pathways. Also, the human plasma proteome is continually undergoing increased refinement as is the human platelet proteome.[5] Essential to the spatiotemporal prediction of clotting or bleeding events is the multiscale modeling of hemodynamic effects that regulate blood function, either through physical forces or mass transfer phenomena.

PLATELETS AND COAGULATION

Platelet Signaling

At the site of plaque rupture or vessel injury, flowing platelets are captured by surface-bound von Willebrand Factor (vWF) followed by engagement of platelet GPVI to collagen leading to calcium mobilization. Calcium mobilization is the central "node" of platelet signaling. During thrombosis, platelets respond simultaneously to collagen binding to GPVI and $\alpha_2\beta_1$, ADP activation of P2Y$_1$, P2Y$_{12}$, and P2X$_1$, epinephrine activation of α_{2A} receptor, thromboxane activation of TP receptor, and thrombin activation of PAR1 and PAR4, while endothelial production of NO

Address correspondence to S. L. Diamond, Department of Chemical and Biomolecular Engineering, Institute for Medicine and Engineering, 1024 Vagelos Research Laboratory, University of Pennsylvania, Philadelphia, PA 19104, USA. Electronic mail: sld@seas.upenn.edu

and prostacyclin (PGI$_2$) dampen responsiveness. Purvis *et al.*[57] developed an ODE model of calcium mobilization and phosphoinositide metabolism following ADP stimulation of the platelet P2Y$_1$ receptor in the absence of extracellular calcium (no store operated calcium entry, SOCE). The model (77 reactions, 132 fixed kinetic rate constants from literature, and 70 species) comprised four interlinked kinetic modules (see Fig. 1). The model accurately predicted: (1) steady-state resting concentrations for Ca$_i$, IP$_3$, DAG, phosphatidic acid, PI, PIP, and PIP$_2$; (2) transient increases in intracellular calcium, IP$_3$, and G$_q$-GTP in response to ADP; and (3) the volume of the platelet dense tubular system (DTS). The initial condition for the 70 intracellular species is largely unknown. However, some species are known in resting platelets and the remaining species are thus highly constrained by topology and known kinetic rate constants. The "homeostasis constraint" requires that the initial condition is a steady state with resting calcium and resting IP$_3$ levels. Purvis *et al.*[58] detailed the use of the homeostasis constraint to find steady states for individual modules and then built a global steady state (and initial condition) from the module steady states. Such an initial condition must also allow for calcium mobilization upon GPCR activation. A successful test of the P2Y$_1$ model involved stochastic simulation of an individual platelet that displayed asynchronous calcium spiking behavior in response to ADP. The model demonstrated that asynchronous spiking was a consequence of stochastic kinetics at the single cell level (noting that 1 nM = ~3 molecules in a 8-fL platelet).

A similar ODE approach was taken to model calcium regulation by stimulation of the PAR1 receptor to activate Akt, PKC, CalDAG-GEF, $\alpha_{2b}\beta_3$, and dense granule release.[41] SOCE *via* STIM1-Orai1 activation following depletion of the DTS store remains to be added to any realistic kinetic model of calcium mobilization.

To account for combinatorial stimulation of numerous receptors, Chatterjee *et al.*[8] developed a 384-well plate assay termed "pairwise agonist scanning (PAS)" to measure platelet calcium mobilization in response to single and pairwise agonist stimulation using an agonist probe set for activation of P2Y$_1$, P2Y$_{12}$, PAR1, PAR4, TP, IP, and GPVI pathways, each used at 0.1×, 1×, and 10× EC$_{50}$. With 154 measured calcium traces to train a 2-layer neural network model, the response of platelets to sequential stimulation and response to 3–6 agonists was accurately predicted. Such data-trained neural network models are patient-specific and ideal for embedding in multiscale flow simulations as described in the next section.
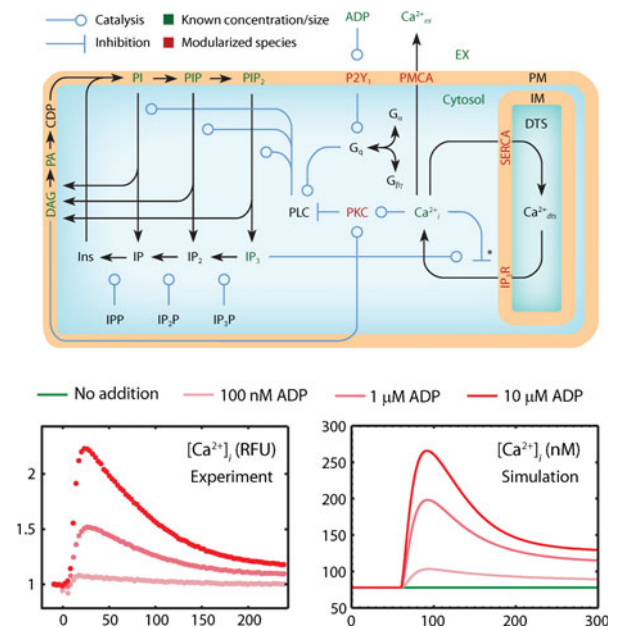

FIGURE 1. Platelet signaling following P2Y1 activation by ADP. ADP binding to P2Y1 triggers G-protein activation through Gq protein leading to the activation of phospholipase C which cleaves PIP2 to release diacylgylcerol (DAG) and inositol trisphosphate (IP$_3$). IP3 receptor (IP3R) channels release Ca$_i$ from the DTS and are regulated biphasically by IP3 and Ca$_i$. The Ca$_i$ is pumped across the PM into the extracellular space (PMCA) or into the DTS using a sarcoplasmic/ER Ca$_i$ ATPase (SERCA). Submodels for IP3R, SERCA, PKC translocation, PKC-mediated feedback inhibition of PLC, and P2Y1 activation are not shown.[57] The full signaling model accurately predicts the dynamics and dose–response of calcium release by ADP-stimulated platelets.

Coagulation

The generation of thrombin by prothrombinase (XaVa) is controlled by the production of Factor Xa through the action of tissue factor/Factor VIIa (TF/VIIa, the "extrinsic tenase") or IXa/VIIIa (formally referred to as the "intrinsic tenase"). Biomaterial activation of the contact pathway (XIIa → XIa → IXa) leads to the generation of IXa/VIIIa; however, IXa can also be generated by TF/VIIa. A number of detailed ODE kinetics models have been developed to describe the generation of thrombin. The Hockin–Mann model is a pseudo-homogeneous model that assumes a fully activated platelet at $t = 0$ with no limitation of platelet phosphatidylserine surface.[31] The model does not distinguish between soluble species and platelet-bound species. The Hockin–Mann model accurately describes thrombin generation in plasma or blood when exogenous TF is added to blood, however it ignores the contact pathway (Factor XIIa) and does not allow thrombin production if initial TF = 0. This model has also been solved stochastically to describe

clotting in small volumes to determine the probability of clotting at low TF levels.[47] More recently, Chatterjee et al.[7] extended the Hockin–Mann model to include the contact pathway and thrombin-mediated feedback activation of resting platelets. This "platelet-plasma" model coarse grains platelet activation and remains a pseudo-homogeneous model, but predicted the clotting of whole blood in the presence or absence of added TF as well as when VIIa, IXa, IXa, and Xa were titrated into blood. Bungay et al.[6] developed a 73-equation ODE model ("Bungay–Gentry" model) with 28 fluid phase species and complexes and 44 lipid bound factors and complexes. This heterogeneous model specifically accounts for the role of lipid surface area during isotropic coagulation (no flow) triggered by TF and allows various factors to compete for available non-specific lipid binding sites.

Kuharsky and Fogelson[39] developed a heterogeneous kinetic model of thrombin generation where coagulation factors bind activated platelets. In contrast to the Bungay–Gentry model, specific lipid binding sites are defined for each species, whereby species do not compete for available lipid. The Kuharsky–Fogelson model was specialized for use with wall-bound TF exposed in a wound patch near endothelium with activated protein C (APC) generating capacity (see next section for further discussion of this model). This model was recently extended to include thrombin-mediated feedback activation of XIa.[26] The Kuharsky–Fogelson model was extended to 92 proteins and 148 interactions by Luan et al.[49] to calculate regulatory linkages in the network topology that exert strong susceptibility to pharmacological inhibition, termed "fragility," that correlated well with actual drug development (including direct Xa and thrombin inhibitors). Haynes et al.[29,30] used a convection–diffusion–reaction model to predict the production of thrombin and factor Xa by surface lipid-bound pro-thrombinase and extrinsic tenase, respectively. While Xa production was found to be transport limited when only extrinsic tenase was present, competition between prothrombinase and extrinsic tenase for lipid binding sites caused Xa production to enter an intermediate regime between reaction and transport limitation.

Highly relevant to biomedical device design, the contact pathway activation of Factor XII to XIIa has been modeled by several groups.[28,35,76] Contact pathway modeling remains quantitatively challenging with respect to defining: (1) mechanism(s) of platelet activation of the contact pathway during in vivo thrombosis, and (2) a priori prediction of XIIa activation kinetics based on biomaterial chemistry.

PHYSICAL CONSIDERATIONS (FROM LARGE TO SMALL SCALES)

Hemodynamics

Large scale finite element calculations provide quantification of complex 3D and transient flows through: bifurcations,[67] stenoses,[4,43] carotid and coronary vessels,[13,56] human and mechanical heart valves,[19] stents,[66] and surgical end-to-side anastomoses.[48] Such simulations often deploy deformable wall boundary conditions, anatomies derived from medical imaging, and complex oscillatory input flows. In the important case of coronary artery stenosis, a 50% stenosis produces little pressure drop and is dangerously asymptomatic, whereas >75% stenosis can produce resistance to flow and generate symptoms of angina. Wall shear rates (γ_w) in a severe stenosis may range from 5000 to >50,000 s^{-1}.[43]

Cellular Level Transport Dynamics

The rheological properties of flowing blood are largely determined by the motion of red blood cells (RBCs) within the vessel. The large deformability of RBCs leads to complex motion in shear flow including tumbling, tank treading, and migration away from the walls. The migration of RBCs away from the wall leads to a cell-free layer, which is composed of plasma and other blood cells including platelets and neutrophils. The extent of the cell-free layer affects the macroscopic viscosity, where a relatively large cell-free layer in smaller vessels corresponds to a drop in viscosity. This is known as the Fahraeus–Lindqvist effect. At vessels much smaller than the RBC diameter, the viscosity increases quickly due to confinement of RBCs. Several groups have developed immersed boundary[2] and discrete particle[21] models that predict the complex cellular motion and viscosity relationships.[15,22] The apparent diffusivity (i.e., dispersivity) of platelets is increased by orders of magnitude above the expected Brownian diffusivity due to the presence of RBC motion.[68] Platelets also become concentrated by ~3–8-fold near the wall,[1,74] the exact location where they execute their function upon vessel injury. The increase in platelet concentration has been modeled with continuum models based on radial drift[20] and an extended convection diffusion model.[33] These models require knowledge of either the platelet or RBC concentration profiles. Simulations with flexible RBCs and stiff platelets have directly predicted the near-wall excess of platelets due to RBC motion.[12,75]

Cellular Membrane and Molecular Biomechanics

Threshold levels of flow at wall shear rate, $\gamma_w \sim 100$ s^{-1} (wall shear stress of $\tau_w \sim 1$ dyne/cm^2) are required for platelet GPIb binding to vWF,[16] similar to the "hydrodynamic thresholding" observed for neutrophil PSGL-1 binding to P- or L-selectin.[57,73] The unexpected flow enhancement of platelet translocation on vWF at $\sim$100 s^{-1} may involve: enhanced rotational motion facilitating bonding, membrane tether pulling and deformation, cellular deformation with enhanced contact area, and/or catch-bonding at the molecular bond interface.

The Bell model is an empirically useful approach for characterizing force sensitivity of bond lifetimes where $k_{off} = k_{off}(0) \exp(rF_B/k_B T)$ where k_{off} is the dissociation constant, F_B is the force on the bond, $k_{off}(0)$ is the unstressed off-rate, r is empirically measured reactive compliance, and k_B and T are the Boltzmann constant and temperature, respectively. The colloidal stability of normal blood (plasma vWF does not spontaneously aggregate platelets *in vivo*) and the rapid rolling of platelets on vWF surfaces is fully consistent with the measured short half-life of the GPIb-vWF A1 domain interaction of <1 s. Using pause time analysis, Doggett *et al.*[16] found the platelet GPIb-vWF A1 domain interaction to display slip-bond kinetics [Bell parameters $k_{off}(0) = 3.45$ s^{-1} and $r = 0.016$ nm] for loadings above 30 pN per bond. Reports of recombinant GPIb-vWF A1 domain unstressed lifetimes lasting >100 s[37] are difficult to reconcile with the ease of platelet rolling at 100 s^{-1} where the force on a single platelet is less than $\sim$10 pN (Also see Fig. 2B of Doggett *et al.*[16] of rapid dissociation of translocating platelets from sorbed plasma vWF when flow was decreased to 0.3 dyne/cm^2).

Along with models of vWF unfolding, the use of slip, catch-slip, or flex-bond kinetics awaits validation *via* multiscale adhesive dynamic simulation[53] to predict platelet thresholding, rolling velocities, and shear induced platelet aggregation. Interestingly, the appearance of shear enhanced bonding (catch bonding) can appear in multivalent systems[46] and molecularly flexible systems[9] even when slip bonds are deployed in the model. In terms of cell rheology, membrane tethering[36] and cell deformation[34] during shear exposure can shield bonds from hemodynamic force loading. Additionally, pathological shear rates can drive platelet membrane tether formation.[18,59]

Litvinov *et al.*[45] found two bound states for fibrinogen binding to $\alpha_{2b}\beta_3$ (short duration and long duration). They report that the $\alpha_{2b}\beta_3$-fibrinogen interaction behaves as a classical slip bond in the range of 5–50 pN of pulling force [Bell model parameters of $k_{off}(0) = 0.052$ s^{-1} and $r = 0.28$ nm]. No measurements of $\alpha_2\beta_1$-collagen bond strength are yet available. For multi-scale modeling of thousands of platelets depositing in a thrombus *via* multiple bond types, coarse graining methods will be required to overcome the computational expense of full adhesive dynamics simulations.

Shear Induced Platelet Activation (SIPA), VWF Fibril-Aggregates, and ADAMTS13

Blood or platelet rich plasma exposed to pathologically high shear forces of >5000 s^{-1} for $\sim$1 min in cone-and-plate viscometers will display platelet activation. This process is VWF-dependent and involves shear-dependent modulation of the A1 domains along with GPIb mechanotransduction leading to granule release of ADP.[38,51,52] The recognition that ultralarge VWF (uLVWF) is elevated in TTP patients[10] led to the eventual discovery of ADAMTS13,[42] the plasma processing enzyme that cleaves uLVWF in the presence of shear flow, endothelium, or platelets.[17,62]

Using a recirculating, open-air flow driven by piezoelectric vibration (acoustic streaming), Schneider *et al.*[60] demonstrated a critical shear rate γ_{crit} of >5000 s^{-1} was needed to extend globular VWF to a stretched conformation that can be relaxed back in $\sim$200 ms when flow decreases below γ_{crit}. The exposure time required to extend VWF was not reported. Follow-up studies used 10–20$\times$ physiologic levels of VWF (200 μg/mL) exposed to "high shear" for a "few minutes" to create VWF fibril-aggregates.[65] From these studies, it is difficult to predict what plasma VWF does under acute stenotic exposures that last <10 ms. Using 1 min perfusion of 50 μg/mL VWF over collagen in flow chambers at 35 dyne/cm^2 ($\sim$5000 s^{-1}), Barg *et al.*[3] detected extensive surface-generated VWF fibers, but this did not occur at 5 μg/mL VWF. Shankaran *et al.*[61] used light scattering of pre-sheared VWF (100 μg/mL) to detect 32×10^6 MW aggregates (2155 s^{-1} for 30 s) or 847×10^6 MW aggregates (6000 s^{-1} for 120 s). Importantly, they reported these aggregates were stable for up to 5 h after shear, but were immediately destroyed by 0.1% SDS. Interestingly, conditions of severe aortic stenosis (118 dyne/cm^2) result in depletion of the largest multimers of vWF to yield an acquired von Willebrand disease.[69] Acquired von Willebrand disease also occurs with high speed continuous Left Ventricular Assist Device (LVAD) pumps. Recently, Nesbitt *et al.*[54] proposed that a shear gradient-dependent platelet aggregation drives thrombus formation whereby discoid platelets cluster downstream of a blockage ($\gamma_w \sim 20{,}000$ s^{-1}) *via* platelet membrane tethering and GP1b mediated adhesion to VWF.

MULTISCALE MODELS OF THROMBOSIS

Multiscale simulation of thrombosis seeks to integrate transport processes, platelet biology, coagulation biochemistry, and bond mechanics. Hubbell and McIntire developed a continuum convection–diffusion–reaction model to describe the concentration profiles of ADP, TXA_2, and thrombin for a given thrombus "patch" on the surface of a parallel plate.[32] To derive the rate of agonist release at the surface, various thrombus sizes, platelet densities, and platelet fluxes were prescribed on the thrombus patch. TXA_2 and thrombin were both enzymatically generated, and the rate of generation of each was assumed to depend on the density of platelets currently on the patch. In contrast, platelets store a finite amount of ADP that is released upon activation, so the rate of generation was assumed to be dependent on the rate of platelet deposition but not on the current platelet density. They computed concentration profiles for these agonists at 100, 500, and 1500 s^{-1} to predict typical boundary layer concentrations of [ADP] = 0.5 μM, [TXA2] = 25 nM, and [thrombin] = 5 U/mL. Folie and McIntire[27] extended this analysis to include geometries other than thrombus "patches" on the surface including rectangular shaped clots and circular clots that protrude into the lumen of the vessel. Also, the effect of having a second thrombus at different downstream lengths was investigated where the formation of a standing vortex is possible. The recirculation regions were found to be zones of high agonist accumulation especially for closely neighboring clots. These approaches, however, do not predict the dynamics of clot growth (Table 1).

Sorensen et al.[63,64] coupled platelet deposition to the release of platelet agonists at the surface. Platelets are modeled as a continuum species that can become activated by local concentrations of the agonists ADP, TXA_2, and thrombin. The generation rate and transport of these agonists was handled similarly to the McIntire models. Platelet activation and platelet deposition were modeled as separate reactions. Two types of platelet species exist, resting and activated platelets. Resting platelets were converted to activated platelets by one of two mechanisms. Adhesion of a resting platelets to the wall can directly activate some percentage of the resting platelets. Resting platelets can also be activated by an accumulation of the local platelet agonists. The weighted sums of the concentration of local agonists are used to define a threshold for the activation step, and above this threshold, the rate of activation becomes nonzero and increases linearly. The density and flux of platelets to the surface is then used to calculate the fluxes of agonists. The coupled model predicted platelet densities for Poiseuille flow over a long collagen surface (1 cm) with and

TABLE 1. Overview of multiscale models.

Model	Physical and biological phenomena	Methods	References
Hubbell/McIntire and Folie/McIntire	ADP, TXA_2, and thrombin transport	Continuum convection–diffusion–reaction equation	27, 32
Sorensen et al.	Agonist release (ADP, TXA_2 and thrombin) and platelet deposition	Continuum convection–diffusion–reaction equation	63, 64
Kuharsky and Fogelson	Thrombin production (coagulation cascade) and platelet deposition	Well-mixed boundary layer (continuum) with no dependence on space	39
Leiderman and Fogelson	Thrombin (coagulation cascade) production, ADP release, and platelet deposition	Spatially resolved convection–diffusion–reaction equations for species (including platelets) transport/generation and Navier–Stokes equations for fluid flow	40
Xu et al.	Thrombin (coagulation cascade) production, ADP and TXA_2 release, and platelet deposition	Cellular Potts model for platelet deposition, convection–diffusion–reaction equation for species transport/generation, and Navier–Stokes equations for fluid flow	70–72
Flamm et al.	ADP and TXA_2 release, platelet deposition, donor-specific platelet signaling	LKMC for platelet deposition, convection–diffusion–reaction equation for species transport/generation, lattice Boltzmann for fluid flow, and neural network for cellular signaling	23

without different anticoagulant therapies. The predictions were directly compared to experimental measurements of platelet density. Furthermore, the model predicted the changes in the concentrations of ADP and TXA_2 due to inhibition of thrombin, which was only feasible by coupling platelet deposition and agonist generation/release.

Although the Sorensen and McIntire models compute thrombin concentration profiles, the flux of thrombin generation was prescribed per platelet and only a few species need to be tracked computationally (prothrombin, thrombin, antithrombin-III, *etc.*). The first model to comprehensively consider the coagulation cascade in flowing blood was developed by Kuharsky and Fogelson.[39] Instead of solving the spatially varying concentration profiles of each enzyme in the cascade, the reactions were assumed to occur in a thin, well-mixed region near the injured surface. Transport of the active species from the injury site into the bulk flow of whole blood was determined by a mass transfer coefficient, which captures the effect of both flow and diffusion. This approach allowed for the solution of >50 ODEs including plasma-phase enzymes, membrane-phase enzymes and enzyme complexes instead of solving the full spatial problem consisting of partial differential equations. Binding of cofactors in the plasma phase and on the membranes of platelets was explicitly considered within the model in response to the exposure of tissue factor at the surface. Platelets are considered as a continuum species that can be activated by thrombin and by other activated platelets, and activated platelets serve as a source for membrane reactions. The specific form of the activation function is a Hill function with an exponent of 1, thus differing from the Sorensen *et al.* model, which used a linear increase above a threshold. The authors found a very sharp threshold for thrombin production while varying TF density, i.e., the concentration of thrombin changed many orders of magnitude in response to a small change in TF density (factor of 2). The threshold was observed at approximately 10–15 fmol/cm^2 and was weakly sensitive to changes in flow. A sharp TF threshold was observed experimentally in flowing whole blood between 1 and 10 TF molecules/μm^2.[55] To achieve a reduction in thrombin production in hemophilia A and B, a new mechanism for inhibition of subendothelial TF:VIIa was proposed whereby deposited platelets physically inhibit the function of the extrinsic tenase. Therefore, platelet activation and deposition acts as a feed-forward mechanism by providing more active surface for thrombin production and an inhibitor of thrombin production by inhibiting extrinsic tenase on the subendothelium. In normal plasma, the production of intrinsic tenase (VIIIa:IXa) is able to sustain thrombin production, while in

hemophilia, the driving force is the transient TF:VIIa exposure.

One complication of embedding the roles of convection and diffusion into a mass transfer coefficient is that the reaction volume, or alternatively the height, of the well-mixed region depends on the flow velocity.[14] When converting a surface density to a volumetric concentration within the well-mixed region, the effective concentrations now depend on the flow physics. Another limitation of this method is that the size and morphology of the clot[11] cannot be determined.

Leiderman and Fogelson[40] extended the Kuharsky–Fogelson model by considering a spatially varying system. In addition to the generation/consumption equations for each species in the model, transport by convection and diffusion is also considered at every position in the fluid. Platelets are still considered a continuum species, but the transport of platelets is now affected by the presence of bound platelets in the same fluid region. To include the effect of particle size, an extra species, denoted by η, that is released from thrombus-bound platelets is tracked. The η species diffuses and is consumed by a first order reaction so that the concentration is high only on the order of one platelet diameter away. Thus, the concentration of η allows for the system to include the physical size of platelets within the system. The effect of platelet buildup on the flow field was introduced using a Brinkman term in the Navier–Stokes equations, which effectively slows down the fluid through regions containing bound platelets. Another addition to the model is the release of ADP, another platelet agonist. The activation kinetics of platelets by ADP and thrombin have the same functional form as in Kuharsky–Fogelson model. The coagulation cascade also includes some additional mechanisms such as inhibition through tissue factor pathway inhibitor (TFPI) and APC. The Leiderman–Fogelson model displayed slightly lower TF threshold as compared to the Kuharsky–Fogelson model. The spatial model predicted that a near-wall excess of platelets, which is created by RBC motion, was required to obtain appreciable platelet deposition. Although RBC motion was not considered explicitly in this model, the effect of shear rate on platelet margination was investigated by probing the model with various combinations of inlet concentration profiles and shear rates. Flow velocity of plasma through the porous clot exhibited a minimum, and the time of the minimum coincided with the "appearance" of thrombin in the simulation. The model also predicted the spatial distributions of platelet density and enzymatic complexes as well as the changes in intra-thrombus flow.

In a particle-explicit approach, Xu *et al.*[70–72] tracked the positions and shapes of platelets moving in a flow

with a cellular Potts model to predict platelet deposition and clot morphology. A cellular Potts model discretizes the space such that each platelet occupies a set of neighboring nodes on the lattice. Other lattice nodes can be occupied by fluid or other cell types, e.g., RBCs. The system is evolved by making random identity switches, for example a fluid node might become occupied by a nearby platelet. The "energy" of the system is computed before and after the switch, and the move is accepted according the Metropolis Monte Carlo acceptance criterion. The energy term includes flow velocity effects, cellular bonding, and cell volume (area in 2D) constraints. Platelet activation was assumed to occur instantaneously after a threshold level of agonist (or sums of agonists) was encountered.[70,71] Platelet activation also occurred directly by interacting with the surface and other activated platelets.[72] Porous flow was computed using Darcy flow within the clot while the bulk blood flow was solved with the Navier–Stokes equations. The production of thrombin was determined with a modified spatial version of the Kuharsky–Fogelson model including the effect of Factor XI feedback. The cellular-Potts model predicted platelet density at different flow rates with and without pulsatility. In general, clot size exhibited a maximum at an intermediate flow rate, which was insensitive to changes in porosity and blood viscosity. Consistent with results from a laser-injury mouse model, the simulation predicted an initial rise in clot volume followed by a reduction to a stable value. One drawback of the cellular Potts model is that the energy parameters of the model do not necessarily correspond to physical (and thus measurable) quantities. Certain parameters such as the volume constraint affect cell motion, which couples these parameters together.

Flamm *et al.*[24] used a lattice kinetic Monte Carlo (LKMC) simulation to predict stochastic particle convection–diffusion and bulk aggregation of stochastic particles in complex shear fields.[25] Similar to the cellular Potts model, the LKMC model resolves cells on a lattice to simulate particle motion in the fluid and aggregation to collagen or deposited platelets. LKMC directly captures the kinetics in the system including cellular motion and aggregation, and the parameters can be directly compared to physical quantities. In considering ADP and TXA_2 release kinetics (no thrombin generation) from activated platelets, concentration boundary layers were simulated by finite element methods. Platelet activation kinetics due to these agonists were derived directly from high-throughput experiments using a neural network model to interpolate and extrapolate from the experimental conditions[8] for platelets stimulated in dilute platelet rich plasma (normal extracellular calcium). The experimental results and thus the neural networks were specific to a single patient. The neural network was embedded into each platelet in the computational domain to determine the activation state from the history of agonist exposure. The kinetics of binding and unbinding from the surface were derived from each platelet's individual activation state. The velocity field of the blood was determined using the lattice Boltzmann method. The clot was assumed to exclude flow, so only diffusive transport of the soluble agonists occured within the clot structure. The results were directly compared to microfluidic measurements[11,50] of platelet deposition onto a collagen surface with various inhibitors of platelet function: iloprost (prostacyclin mimic), aspirin or indomethacin (COX-1 therapy), and MRS-2179 (P2Y$_1$ inhibitor). The shear rate distribution and the concentrations of ADP and TXA_2 were highly heterogeneous in the simulations (see Fig. 2a). For three unique donors, the model predicted that iloprost treatment led to the largest reduction in platelet deposition, aspirin treatment led to the smallest reduction, and MRS 2179 had a medium reduction in platelet deposition (see Figs. 2b and 2c). The same ranked order was also observed in the experiment. The model also predicted that one of the donors had significantly larger clots than the other two donors, and another donor was insensitive to anti-COX-1 therapy, which was also consistent with experiment. The anti-COX-1 resistance was found to be caused by a novel mutation in the TP receptor of that donor. The model also predicted strong fluctuations in ADP concentration that was linked to the short burst of ADP release upon platelet activation. TXA_2 did not exhibit fluctuations, since it was enzymatically generated over a longer time period.[23]

SUMMARY

The hierarchical nature from molecular receptor–ligand mechanics to cell signaling to clot formation progresses across several highly coupled length and time scales. A number of teams have pushed the quantitative frontier of single molecule bond dynamics, vWF polymer physics, platelet signaling, coagulation biochemistry, cellular biorheology of blood, and large vessel hemodynamics. Using both continuum and particle based simulation tools, multiscale simulations of thrombosis can be now be tuned to patient-specific coagulation and platelet function (in the presence of pharmacological modifiers) for patient-specific three dimensional vascular geometries. Model scale will approach $O(10^1–10^2)$ physics-based parameters, $O(10^2–10^3)$ chemical species, and $O(10^2–10^3)$ kinetic parameters, requiring $10^2–10^4$ CPU hours per simulation. Validation of such large models continues to rely
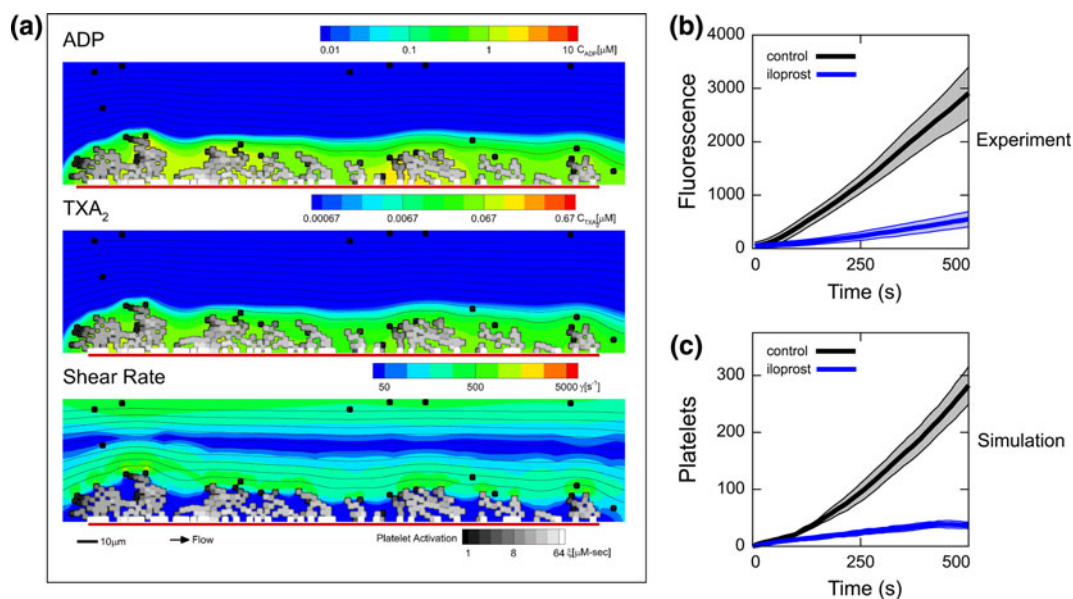
FIGURE 2. Multiscale simulation of platelet deposition under flow. (a) Platelet deposition to a collagen patch on the surface in the presence of ADP (top) and TXA$_2$ (middle) where flow is from left to right. The local shear rate (bottom) at the platelet deposit surface has a large range (<50 to >1000 s^{-1}) due to the heterogeneous platelet density. The color of each platelet represents the activation state (white, activated; black, unactivated). (b) Microfluidic experiment of platelet deposition to a collagen patch with and without iloprost, an IP agonist. Iloprost mimics the function of the physiological anti-platelet molecule prostacyclin, which is emitted by unactivated endothelial cells. Thick lines, mean fluorescence for control (black) and platelets treated with iloprost (blue); shaded area, standard deviation. (c) Multiscale prediction of platelet deposition to collagen patch with and without iloprost. Thick lines, mean platelet number on patch for control (black) and platelets treated with iloprost (blue); shaded area, standard deviation.

on passing certain tests: prediction of severity of genotype/phenotype linkages (hemophilia, APC resistance, *etc.*), drug sensitivity, and *in vitro* microfluidic tests where numerous blood factors are modulated. Such models, beyond their use in helping to resolve purely scientific issues of kinetic significance of various pathways, offer the future in personalized medicine to predict patient-specific disease risks, sensitivity to pharmacological intervention, and risks of side effects. Multiscale models of blood also have utility in biomedical device design. In complex and multifactorial clinical situations such as trauma or massive surgical bleeding, a multiscale approach may help predict improved patient outcomes for different therapeutic approaches.

REFERENCES

[1]Aarts, P. A., S. A. van den Broek, G. W. Prins, G. D. Kuiken, J. J. Sixma, and R. M. Heethaar. Blood platelets are concentrated near the wall and red blood cells, in the center in flowing blood. *Arterioscler. Thromb. Vasc. Biol.* 8:819–824, 1988.

[2]Bagchi, P. Mesoscale simulation of blood flow in small vessels. *Biophys. J.* 92:1858–1877, 2007.

[3]Barg, A., R. Ossig, T. Goerge, M. F. Schneider, H. Schillers, H. Oberleithner, and S. W. Schneider. Soluble plasma-derived von Willebrand factor assembles to a halemostatically active filamentous network. *Thromb. Haemost.* 97:514–526, 2007.

[4]Bathe, M., and R. D. Kamm. A fluid–structure interaction finite element analysis of pulsatile blood flow through a compliant stenotic artery. *J. Biomech. Eng.* 121:361–369, 1999.

[5]Boyanova, D., S. Nilla, I. Birschmann, T. Dandekar, and M. Dittrich. PlateletWeb: a systems biologic analysis of signaling networks in human platelets. *Blood* 119:e22–e34, 2011.

[6]Bungay, S. D., P. A. Gentry, and R. D. Gentry. A mathematical model of lipid-mediated thrombin generation. *Math. Med. Biol.* 20:105–129, 2003.

[7]Chatterjee, M. S., W. S. Denney, H. Jing, and S. L. Diamond. Systems biology of coagulation initiation: kinetics of thrombin generation in resting and activated human blood. *PLoS Comput. Biol.* 6:e1000950, 2010.

[8]Chatterjee, M. S., J. E. Purvis, L. F. Brass, and S. L. Diamond. Pairwise agonist scanning predicts cellular signaling responses to combinatorial stimuli. *Nat. Biotechnol.* 28:727–732, 2010.

[9]Chen, H., and A. Alexander-Katz. Polymer-based catchbonds. *Biophys. J.* 100:174–182, 2011.

[10]Chintagumpala, M. M., R. L. Hurwitz, J. L. Moake, D. H. Mahoney, and C. P. Steuber. Chronic relapsing thrombotic thrombocytopenic purpura in infants with large von Willebrand factor multimers during remission. *J. Pediatr.* 120:49–53, 1992.

[11]Colace, T., E. Falls, X. Zheng, and S. Diamond. Analysis of morphology of platelet aggregates formed on collagen under laminar blood flow. *Ann. Biomed. Eng.* 39:922–929, 2011.

[12]Crowl, L. M., and A. L. Fogelson. Computational model of whole blood exhibiting lateral platelet motion induced by red blood cells. *Int. J. Numer. Methods Biomed. Eng.* 26:471–487, 2010.

[13]Delfino, A., N. Stergiopulos, J. E. Moore, Jr., and J. J. Meister. Residual strain effects on the stress field in a thick wall finite element model of the human carotid bifurcation. *J. Biomech.* 30:777–786, 1997.

[14]Diamond, S. L. Reaction complexity of flowing human blood. *Biophys. J.* 80:1031–1032, 2001.

[15]Doddi, S. K., and P. Bagchi. Three-dimensional computational modeling of multiple deformable cells flowing in microvessels. *Phys. Rev. E* 79:046318, 2009.

[16]Doggett, T. A., G. Girdhar, A. Lawshe, D. W. Schmidtke, I. J. Laurenzi, S. L. Diamond, and T. G. Diacovo. Selectin-like kinetics and biomechanics promote rapid platelet adhesion in flow: the GPIbα-vWF tether bond. *Biophys. J.* 83:194–205, 2002.

[17]Dong, J.-f., J. L. Moake, L. Nolasco, A. Bernardo, W. Arceneaux, C. N. Shrimpton, A. J. Schade, L. V. McIntire, K. Fujikawa, and J. A. Lopez. ADAMTS-13 rapidly cleaves newly secreted ultralarge von Willebrand factor multimers on the endothelial surface under flowing conditions. *Blood* 100:4033–4039, 2002.

[18]Dopheide, S. M., M. J. Maxwell, and S. P. Jackson. Shear-dependent tether formation during platelet translocation on von Willebrand factor. *Blood* 99:159–167, 2002.

[19]Dumont, K., J. Vierendeels, R. Kaminsky, G. van Nooten, P. Verdonck, and D. Bluestein. Comparison of the hemodynamic and thrombogenic performance of two bileaflet mechanical heart valves using a CFD/FSI model. *J. Biomech. Eng.* 129:558–565, 2007.

[20]Eckstein, E. C., and F. Belgacem. Model of platelet transport in flowing blood with drift and diffusion terms. *Biophys. J.* 60:53–69, 1991.

[21]Fedosov, D. A., B. Caswell, and G. E. Karniadakis. A multiscale red blood cell model with accurate mechanics, rheology, and dynamics. *Biophys. J.* 98:2215–2225, 2010.

[22]Fedosov, D. A., W. Pan, B. Caswell, G. Gompper, and G. E. Karniadakis. Predicting human blood viscosity in silico. *Proc. Nat. Acad. Sci.* 108:11772–11777, 2011.

[23]Flamm, M. H., T. Colace, M. S. Chatterjee, H. Jing, S. Zhou, D. Jaegar, L. F. Brass, T. Sinno, and S. L. Diamond. Multiscale prediction of patient-specific platelet function under flow. *Blood* 2012 (in press).

[24]Flamm, M. H., S. L. Diamond, and T. Sinno. Lattice kinetic Monte Carlo simulations of convective-diffusive systems. *J. Chem. Phys.* 130:094904, 2009.

[25]Flamm, M. H., T. Sinno, and S. L. Diamond. Simulation of aggregating particles in complex flows by the lattice kinetic Monte Carlo method. *J. Chem. Phys.* 134:034905, 2011.

[26]Fogelson, A. L., Y. H. Hussain, and K. Leiderman. Blood clot formation under flow: the importance of Factor XI depends strongly on platelet count. *Biophys. J.* 102:10–18, 2012.

[27]Folie, B. J., and L. V. McIntire. Mathematical analysis of mural thrombogenesis. Concentration profiles of platelet-activating agents and effects of viscous shear flow. *Biophys. J.* 56:1121–1141, 1989.

[28]Guo, Z., K. M. Bussard, K. Chatterjee, R. Miller, E. A. Vogler, and C. A. Siedlecki. Mathematical modeling of material-induced blood plasma coagulation. *Biomaterials* 27:796–806, 2006.

[29]Haynes, L. M., Y. C. Dubief, and K. G. Mann. Membrane binding events in the initiation and propagation phases of tissue factor initiated zymogen activation under flow. *J. Biol. Chem.* 287:5225–5234, 2012.

[30]Haynes, L. M., Y. C. Dubief, T. Orfeo, and K. G. Mann. Dilutional control of prothrombin activation at physiologically relevant shear rates. *Biophys. J.* 100:765–773, 2011.

[31]Hockin, M. F., K. C. Jones, S. J. Everse, and K. G. Mann. A model for the stoichiometric regulation of blood coagulation. *J. Biol. Chem.* 277:18322–18333, 2002.

[32]Hubbell, J. A., and L. V. McIntire. Platelet active concentration profiles near growing thrombi. A mathematical consideration. *Biophys. J.* 50:937–945, 1986.

[33]Hund, S. J., and J. F. Antaki. An extended convection diffusion model for red blood cell-enhanced transport of thrombocytes and leukocytes. *Phys. Med. Biol.* 54:6415–6435, 2009.

[34]Jadhav, S., C. D. Eggleton, and K. Konstantopoulos. A 3-D computational model predicts that cell deformation affects selectin-mediated leukocyte rolling. *Biophys. J.* 88:96–104, 2005.

[35]Jesty, J., and E. Beltrami. Positive feedbacks of coagulation. *Arterioscler. Thromb. Vasc. Biol.* 25:2463–2469, 2005.

[36]Kadash, K. E., M. B. Lawrence, and S. L. Diamond. Neutrophil string formation: hydrodynamic thresholding and cellular deformation during cell collisions. *Biophys. J.* 86:4030–4039, 2004.

[37]Kim, J., C.-Z. Zhang, X. Zhang, and T. A. Springer. A mechanically stabilized receptor–ligand flex-bond important in the vasculature. *Nature* 466:992–995, 2010.

[38]Konstantopoulos, K., T. W. Chow, N. A. Turner, J. D. Hellums, and J. L. Moake. Shear stress-induced binding of von Willebrand factor to platelets. *Biorheology* 34:57–71, 1997.

[39]Kuharsky, A. L., and A. L. Fogelson. Surface-mediated control of blood coagulation: the role of binding site densities and platelet deposition. *Biophys. J.* 80:1050–1074, 2001.

[40]Leiderman, K., and A. L. Fogelson. Grow with the flow: a spatial temporal model of platelet deposition and blood coagulation under flow. *Math. Med. Biol.* 28:47–84, 2011.

[41]Lenoci, L., M. Duvernay, S. Satchell, E. DiBenedetto, and H. E. Hamm. Mathematical model of PAR1-mediated activation of human platelets. *Mol. BioSyst.* 7:1129–1137, 2010.

[42]Levy, G. G., W. C. Nichols, E. C. Lian, T. Foroud, J. N. McClintick, B. M. McGee, A. Y. Yang, D. R. Siemieniak, K. R. Stark, R. Gruppo, R. Sarode, S. B. Shurin, V. Chandrasekaran, S. P. Stabler, H. Sabio, E. E. Bouhassira, J. D. Upshaw, D. Ginsburg, and H.-M. Tsai. Mutations in a member of the ADAMTS gene family cause thrombotic thrombocytopenic purpura. *Nature* 413:488–494, 2001.

[43]Li, M. X., J. J. Beech-Brandt, L. R. John, P. R. Hoskins, and W. J. Easson. Numerical analysis of pulsatile blood flow and vessel wall mechanics in different degrees of stenoses. *J. Biomech.* 40:3715–3724, 2007.

[44]Li, Z., M. K. Delaney, K. A. O'Brien, and X. Du. Signaling during platelet adhesion and activation. *Arterioscler. Thromb. Vasc. Biol.* 30:2341–2349, 2010.

[45]Litvinov, R. I., V. Barsegov, A. J. Schissler, A. R. Fisher, J. S. Bennett, J. W. Weisel, and H. Shuman. Dissociation of bimolecular αIIb–b3–fibrinogen complex under a constant tensile force. *Biophys. J.* 100:165–173, 2011.

[46]Liu, J., N. J. Agrawal, A. Calderon, P. S. Ayyaswamy, D. M. Eckmann, and R. Radhakrishnan. Multivalent binding of nanocarrier to endothelial cells under shear flow. *Biophys. J.* 101:319–326, 2011.

[47]Lo, K., W. S. Denney, and S. L. Diamond. Stochastic modeling of blood coagulation initiation. *Pathophysiol. Haemost. Thromb.* 34:80–90, 2005.

[48]Loth, F., P. F. Fischer, and H. S. Bassiouny. Blood flow in end-to-side anastomoses. *Annu. Rev. Fluid Mech.* 40:367–393, 2008.

[49]Luan, D., M. Zai, and J. D. Varner. Computationally derived points of fragility of a human cascade are consistent with current therapeutic strategies. *PLoS Comput. Biol.* 3:e142, 2007.

[50]Maloney, S. F., L. F. Brass, and S. L. Diamond. $P2Y_{12}$ or $P2Y_1$ inhibitors reduce platelet deposition in a microfluidic model of thrombosis while apyrase lacks efficacy under flow conditions. *Integr. Biol.* 2:183–192, 2010.

[51]Moake, J. L., N. A. Turner, N. A. Stathopoulos, L. Nolasco, and J. D. Hellums. Shear-induced platelet aggregation can be mediated by vWF released from platelets, as well as by exogenous large or unusually large vWF multimers, requires adenosine diphosphate, and is resistant to aspirin. *Blood* 71:1366–1374, 1988.

[52]Moake, J. L., N. A. Turner, N. A. Stathopoulos, L. H. Nolasco, and J. D. Hellums. Involvement of large plasma von Willebrand factor (vWF) multimers and unusually large vWF forms derived from endothelial cells in shear stress-induced platelet aggregation. *J. Clin. Investig.* 78:1456–1461, 1986.

[53]Mody, N. A., and M. R. King. Platelet adhesive dynamics. Part I: Characterization of platelet hydrodynamic collisions and wall effects. *Biophys. J.* 95:2539–2555, 2008.

[54]Nesbitt, W. S., E. Westein, F. J. Tovar-Lopez, E. Tolouei, A. Mitchell, J. Fu, J. Carberry, A. Fouras, and S. P. Jackson. A shear gradient-dependent platelet aggregation mechanism drives thrombus formation. *Nat. Med.* 15:665–673, 2009.

[55]Okorie, U. M., W. S. Denney, M. S. Chatterjee, K. B. Neeves, and S. L. Diamond. Determination of surface tissue factor thresholds that trigger coagulation at venous and arterial shear rates: amplification of 100 fM circulating tissue factor requires flow. *Blood* 111:3507–3513, 2008.

[56]Perktold, K., and D. Hilbert. Numerical simulation of pulsatile flow in a carotid bifurcation model. *J. Biomed. Eng.* 8:193–199, 1986.

[57]Purvis, J. E., M. S. Chatterjee, L. F. Brass, and S. L. Diamond. A molecular signaling model of platelet phosphoinositide and calcium regulation during homeostasis and P2Y1 activation. *Blood* 112:4069–4079, 2008.

[58]Purvis, J. E., R. Radhakrishnan, and S. L. Diamond. Steady-state kinetic modeling constrains cellular resting states and dynamic behavior. *PLoS Comput. Biol.* 5:e1000298, 2009.

[59]Ruggeri, Z. M., J. N. Orje, R. Habermann, A. B. Federici, and A. J. Reininger. Activation-independent platelet adhesion and aggregation under elevated shear stress. *Blood* 108:1903–1910, 2006.

[60]Schneider, S. W., S. Nuschele, A. Wixforth, C. Gorzelanny, A. Alexander-Katz, R. R. Netz, and M. F. Schneider. Shear-induced unfolding triggers adhesion of von Willebrand factor fibers. *Proc. Nat. Acad. Sci.* 104:7899–7903, 2007.

[61]Shankaran, H., P. Alexandridis, and S. Neelamegham. Aspects of hydrodynamic shear regulating shear-induced platelet activation and self-association of von Willebrand factor in suspension. *Blood* 101:2637–2645, 2003.

[62]Shim, K., P. J. Anderson, E. A. Tuley, E. Wiswall, and J. Evan Sadler. Platelet–VWF complexes are preferred substrates of ADAMTS13 under fluid shear stress. *Blood* 111:651–657, 2008.

[63]Sorensen, E. N., G. W. Burgreen, W. R. Wagner, and J. F. Antaki. Computational simulation of platelet deposition and activation: I. Model development and properties. *Ann. Biomed. Eng.* 27:436–448, 1999.

[64]Sorensen, E. N., G. W. Burgreen, W. R. Wagner, and J. F. Antaki. Computational simulation of platelet deposition and activation: II. Results for Poiseuille flow over collagen. *Ann. Biomed. Eng.* 27:449–458, 1999.

[65]Steppich, D. M., J. I. Angerer, K. Sritharan, S. W. Schneider, S. Thalhammer, A. Wixforth, A. Alexander-Katz, and M. F. Schneider. Relaxation of ultralarge VWF bundles in a microfluidic–AFM hybrid reactor. *Biochem. Biophys. Res. Commun.* 369:507–512, 2008.

[66]Stuhne, G. R., and D. A. Steinman. Finite-element modeling of the hemodynamics of stented aneurysms. *J. Biomech. Eng.* 126:382–387, 2004.

[67]Taylor, C. A., T. J. R. Hughes, and C. K. Zarins. Finite element modeling of three-dimensional pulsatile flow in the abdominal aorta: relevance to atherosclerosis. *Ann. Biomed. Eng.* 26:975–987, 1998.

[68]Turitto, V. T., A. M. Benis, and E. F. Leonard. Platelet diffusion in flowing blood. *Ind. Eng. Chem. Fundam.* 11:216–223, 1972.

[69]Vincentelli, A., S. Susen, T. Le Tourneau, I. Six, O. Fabre, F. Juthier, A. Bauters, C. Decoene, J. Goudemand, A. Prat, and B. Jude. Acquired von Willebrand syndrome in aortic stenosis. *N. Engl. J. Med.* 349:343–349, 2003.

[70]Xu, Z., N. Chen, M. M. Kamocka, E. D. Rosen, and M. Alber. A multiscale model of thrombus development. *J. R. Soc. Interface* 5:705–722, 2008.

[71]Xu, Z., N. Chen, S. C. Shadden, J. E. Marsden, M. M. Kamocka, E. D. Rosen, and M. Alber. Study of blood flow impact on growth of thrombi using a multiscale model. *Soft Matter* 5:769–779, 2009.

[72]Xu, Z., J. Lioi, J. Mu, M. M. Kamocka, X. Liu, D. Z. Chen, E. D. Rosen, and M. Alber. A multiscale model of venous thrombus formation with surface-mediated control of blood coagulation cascade. *Biophys. J.* 98:1723–1732, 2010.

[73]Yago, T., J. H. Wu, C. D. Wey, A. G. Klopocki, C. Zhu, and R. P. McEver. Catch bonds govern adhesion through L-selectin at threshold shear. *J. Cell Biol.* 166:913–923, 2004.

[74]Yeh, C., and E. C. Eckstein. Transient lateral transport of platelet-sized particles in flowing blood suspensions. *Biophys. J.* 66:1706–1716, 1994.

[75]Zhao, H., and E. S. G. Shaqfeh. Shear-induced platelet margination in a microchannel. *Phys. Rev. E* 83:061924, 2011.

[76]Zhuo, R., C. A. Siedlecki, and E. A. Vogler. Competitive-protein adsorption in contact activation of blood Factor XII. *Biomaterials* 28:4355–4369, 2007.